Learning-Based BBA Modeling Approach with Multi-Method Fusion

Siyuan Li, Deqiang Han
School of Automation Science and Engineering
Xi'an Jiaotong University
Xi'an, Shaanxi, China
15822977756@163.com; deqhan@xjtu.edu.cn

Jean Dezert
The French Aerospace Lab - ONERA
Chemin de la Hunière
F-91761 Palaiseau, France
jean.dezert@onera.fr

Yi Yang
SKLSVMS, School of Aerospace
Xi'an Jiaotong University
Xi'an, Shaanxi, China
jiafeiyy@xjtu.edu.cn

***Abstract*—Dempster-Shafer evidence theory (DST) is a theoretical framework for uncertainty modeling and reasoning, with modeling the basic belief assignment (BBA) as one of its most crucial and challenging tasks. The prevailing BBA determination methods have their own pros and cons, and the joint use of them is expected to provide a better BBA. To realize an end-to-end BBA modeling without explicitly using various prevailing BBA modeling methods, a learning-based BBA modeling approach with multi-method fusion (LBMMF) is proposed in this paper. Deep learning is used to train a deep network which learns the mapping from the training samples to the comprehensive BBAs obtained by jointly using the prevailing BBA modeling methods as the generalized training labels. Given a test sample, the corresponding BBA can be obtained in an end-to-end manner, which is the output of the trained deep neural network. Experimental results show that to use the BBA obtained by our method can achieve better classification performance.**

***Index Terms*—basic belief assignment (BBA), evidence theory, deep learning, pattern classification.**

I. Introduction

The theory of belief functions [1], also called Dempster-Shafer evidence theory (DST), serves as an effective tool for uncertainty modeling and reasoning. DST has been widely used in many real-world problems including object recognition [2], medical diagnosis [3] and intrusion detection [4]. In DST, a crucial and challenging issue is the representation of uncertainty, i.e., the determination of the mass function, also known as the basic belief assignment (BBA). The BBA is a kind of random set in nature and its determination is the problem of modeling the distribution of random set [5], and therefore, the modeling of BBA is difficult and challenging.

Up to now, the existing BBA determination methods can be categorized into two types: the approaches that directly determine BBA from data and the approaches that transform other types of uncertainty representation into BBA.

Several representative approaches that directly determine BBA from data are as follows. Shafer [1] determined BBA based on statistical evidence. Selzer *et al* [6] proposed a method for automatic target classification, taking the class number and the target's neighborhood into account. Valente *et al* [7] proposed a method for determining BBA in the context of speech recognition via combining the outputs from different neural networks. Han *et al* [8] proposed a BBA determination method based on the uncertainty intervals of multiple attributes. Qiu *et al* [9] designed a method for generating BBA specifically for addressing fuzzy time series forecasting problems. Masson *et al* [10] proposed an evidential version of the fuzzy c-means algorithm to determine BBA. Kang *et al* [11] used interval numbers to model each class in the dataset for BBA determination. Based on Kang's approach, Zhang *et al* [12] used triangular fuzzy numbers and trapezoidal fuzzy numbers to model each class in the dataset for BBA determination, since they can preserve more information than the interval number. Tang *et al* [13] proposed a BBA determination method for the incomplete data and information.

There are also some approaches transform other types of uncertainty representation like the fuzzy membership function (FMF) into BBA. For example, Florea *et al* [14] determined BBA from the FMF with focal elements nested in order using α-cut approach. Han *et al* [15] proposed two BBA determination methods from the FMF without predefining focal elements via uncertainty optimization.

The aforementioned BBA determination approaches have their own pros and cons. It should be better if their pros could be promoted while their cons could be prohibited. Obviously, an intuitive approach is to combine the BBAs obtained by these methods; however, such a direct approach lacks efficiency. In this paper, a learning-based BBA modeling approach is proposed to jointly use multiple prevailing BBA determination methods more efficiently, which is called Learning-based Basic belief assignment Modeling with Multi-method Fusion (LBMMF). A deep network is trained to learn the end-to-end modeling of the BBA, which can realize the comprehensive use of their superiority while avoid the explicit use of them at the usage stage. For the deep network training, the inputs are training samples and the outputs are the comprehensive BBAs as the generalized training labels, which are the combination results of the BBAs generated for the training samples by respectively using the prevailing BBA determination methods. The trained deep network is used to determine the BBAs of the test samples in an end-to-end manner. Experimental results show that using LBMMF can achieve better classification performance than using other

This work was supported by National Natural Science Foundation of China, No. U22A2045.

prevailing BBA determination approaches, which demonstrate the effectiveness of our proposed LBMMF.

II. BASICS OF EVIDENCE THEORY

In DST, the frame of discernment (FOD) Θ contains C mutually exclusive and exhaustive elements $\Theta = \{\theta_1, \theta_2, \ldots, \theta_C\}$. The power set of Θ (the set of all subsets of Θ) is denoted by 2^Θ. The basic belief assignment (BBA, also called a mass function) m is defined from 2^Θ to $[0, 1]$ satisfies

$$\sum\nolimits_{A\subseteq\Theta} m(A) = 1, m(\emptyset) = 0 \tag{1}$$

if $m(A) > 0$, A is called a focal element, and $m(A)$ represents the evidence support to A.

Given a BBA on the FOD Θ, the belief function Bel and plausibility function Pl are defined as:

$$Bel(A) = \sum_{B\subseteq A} m(B), \forall A \subseteq \Theta \tag{2}$$

where $Bel(A)$ and $Pl(A)$ constitute the belief interval $[Bel(A), Pl(A)]$, which represents the degree of imprecision for the proposition A.

In the theory of belief functions, the evidence combination is the fusion of the BBAs. Dempster's rule of combination [1] is used for combining two or more independent BBAs.

$$m_{Dempster}(A) = \begin{cases} 0, A = \emptyset \\ \frac{1}{1-K} \sum\limits_{B\cap C=A} m_1(B)m_2(C) A \neq \emptyset \end{cases} \tag{3}$$

where m_1 and m_2 are two independent BBAs on the FOD Θ, and $K = \sum_{B\cap C=\emptyset} m_1(B)m_2(C)$ represents the total conflict or contradictory mass assignments.

Smets *et al* proposed the pignistic probability transformation [16], i.e., $BetP$, to transform a BBA into a probability. The transformation is usually used in the probabilistic decision-making application based on BBA. $BetP$ is defined as:

$$BetP(\theta_i) \triangleq \sum\nolimits_{\theta_i\in A} \frac{m(A)}{|A|}, \forall \theta_i \in \Theta \tag{4}$$

where $|A|$ denotes the cardinality of A. The element in FOD which has the highest $BetP$ value is chosen as the classification result.

III. PREVAILING BBA DETERMINATION METHODS

In this section, several prevailing BBA determination methods are introduced.

For the BBA determination method using interval numbers [11], each dimension of the focal element $A \in \Theta$ is modeled as an interval number $\mathbf{c}_I(A) = [c_{I1}, c_{I2}]$, which is shown in Fig. 1. For a query sample q, it is modeled as an interval number $\mathbf{q}_I = [q, q]$. If the interval number $\mathbf{q}_I$ is near to the interval number $\mathbf{c}_I(A)$, which is the representation of the training data for the focal element A, a larger belief of q belongs to A should be assigned. Consequently, the similarity between $\mathbf{c}_I(A)$ and $\mathbf{q}_I$ is defined as:

$$S_I(\mathbf{c}_I(A), \mathbf{q}_I) = \frac{1}{1 + \alpha_I \cdot d_I(\mathbf{c}_I(A), \mathbf{q}_I)} \tag{5}$$

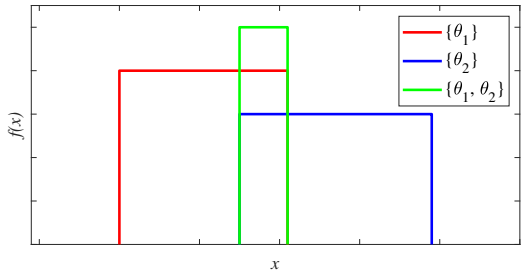

Fig. 1. Representation of focal elements using interval numbers.

$$d_I^2(\mathbf{c}_I(A), \mathbf{q}_I) = \left(q - \frac{c_{I1} + c_{I2}}{2}\right)^2 + \frac{1}{12}(c_{I2} - c_{I1})^2 \tag{6}$$

where α_I is a parameter to control the similarity and $\alpha_I > 0$. $d_I(\mathbf{c}_I(A), \mathbf{q}_I)$ is the distance between $\mathbf{c}_I(A)$ and $\mathbf{q}_I$ [17]. Finally, the similarities are normalized to determine the BBAs.

For the BBA determination method using triangular fuzzy numbers [12], each dimension of the focal element $A \in \Theta$ is modeled as a triangular fuzzy number $\mathbf{c}_T(A) = [c_{T1}, c_{T2}, c_{T3}]$, which is shown in Fig. 2. For a query sample q, it is modeled as a triangular fuzzy number $\mathbf{q}_T = [q, q, q]$. If the triangular fuzzy number $\mathbf{q}_T$ is near to the triangular fuzzy number $\mathbf{c}_T(A)$, which is the representation of the training data for the focal element A, a larger belief of q belongs to A should be assigned. Consequently, the similarity between $\mathbf{c}_T(A)$ and $\mathbf{q}_T$ is defined as:

$$S_T(\mathbf{c}_T(A), \mathbf{q}_T) = \frac{1}{1 + \alpha_T \cdot d_T(\mathbf{c}_T(A), \mathbf{q}_T)} \tag{7}$$

$$d_T^2(\mathbf{c}_T(A), \mathbf{q}_T) = (q - c_{T2})\left[q - \frac{(c_{T1} + c_{T3})}{2}\right] + \frac{1}{9}[(c_{T3} - c_{T2}) - (c_{T2} - c_{T1})]^2 + \frac{1}{9}(c_{T3} - c_{T2})(c_{T2} - c_{T1}) \tag{8}$$

where α_T is a parameter to control the similarity and $\alpha_T > 0$. $d_T(\mathbf{c}_T(A), \mathbf{q}_T)$ is the distance between $\mathbf{c}_T(A)$ and $\mathbf{q}_T$ [17]. Finally, the normalized similarities are used to determine the BBAs.

For the BBA determination method using trapezoidal fuzzy numbers [12], each dimension of the focal element $A \in$

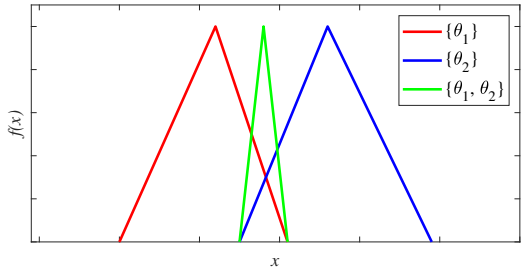

Fig. 2. Representation of focal elements using triangular fuzzy numbers.

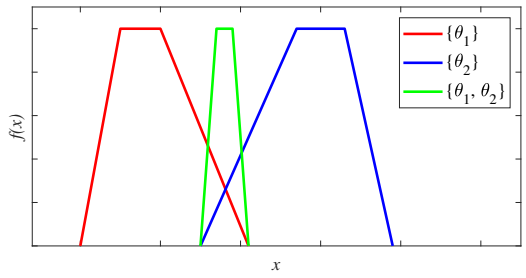

Fig. 3. Representation of focal elements using trapezoidal fuzzy numbers.

Θ is modeled as a trapezoidal fuzzy number $\mathbf{c}_{Tr}(A) = [c_{Tr1}, c_{Tr2}, c_{Tr3}, c_{Tr4}]$, which is shown in Fig. 3. For a query sample q, it is modeled as a trapezoidal fuzzy number $\mathbf{q}_{Tr} = [q, q, q, q]$. If the trapezoidal fuzzy number $\mathbf{q}_{Tr}$ is near to the trapezoidal fuzzy number $\mathbf{c}_{Tr}(A)$, which is the representation of the training data for the focal element A, a larger belief of q belongs to A should be assigned. Consequently, the similarity between $\mathbf{c}_{Tr}(A)$ and $\mathbf{q}_{Tr}$ is defined as:

$$S_{Tr}\left(\mathbf{c}_{Tr}(A), \mathbf{q}_{Tr}\right) = \frac{1}{1 + \alpha_{Tr} \cdot d_{Tr}\left(\mathbf{c}_{Tr}(A), \mathbf{q}_{Tr}\right)} \tag{9}$$

$$d^2_{Tr}(\mathbf{c}_{Tr}(A), \mathbf{q}_{Tr}) = \left[q - \frac{(c_{Tr2} + c_{Tr3})}{2}\right]\left[q - \frac{(c_{Tr1} + c_{Tr4})}{2}\right] + \frac{1}{12}(c_{Tr3} - c_{Tr2})(c_{Tr4} - c_{Tr1}) + \frac{1}{9}(c_{Tr4} - c_{T3})(c_{Tr2} - c_{Tr1}) + \frac{1}{9}\left[(c_{Tr4} - c_{Tr3}) - (c_{Tr2} - c_{Tr1})\right]^2 \tag{10}$$

where α_{Tr} is a parameter to control the similarity and $\alpha_{Tr} > 0$. $d_{Tr}\left(\mathbf{c}_{Tr}(A), \mathbf{q}_{Tr}\right)$ is the distance between $\mathbf{c}_{Tr}(A)$ and $\mathbf{q}_{Tr}$ [17]. Finally, the normalized similarities are used to determine the BBAs.

We also use the BBA generation method in ECM (evidential c-means) [10]. Let $\{x_1, \ldots x_N\}$ be a set of N samples and $C(2 \leq C < N)$ be the number of classes. The centroid $v_k(k = 1, ..., C)$ is used to represent each class. For each sample x_i, ECM can determine the corresponding BBA m_i. The quantity $m_{ij} \triangleq m_i(A_j)$ is obtained in a way that m_{ij} is inversely proportional to the distance d_{ij} between x_i and the focal element A_j. The focal element A_j is represented by a barycenter $\bar{v}_j (1 \leq j \leq 2^C - 1)$, and $\bar{v}_j$ is defined as:

$$\bar{v}_j = \frac{1}{C_j} \sum_{k=1}^{c} s_{kj} v_k \tag{11}$$

where C_j is the number of elements in A_j and

$$s_{kj} = \begin{cases} 1 \text{ if } \theta_k \subseteq A_j \\ 0 \; otherwise. \end{cases} \tag{12}$$

The distance d_{ij} is defined as

$${d_{ij}}^2 = \|x_i - \bar{v}_j\|^2 \tag{13}$$

The BBA can be determined by the following formula:

$$m_{ij} = \frac{C_j^{-\alpha/(\beta-1)} d_{ij}^{-2/(\beta-1)}}{\sum\limits_{A_k \neq \emptyset} C_k^{-\alpha/(\beta-1)} d_{ik}^{-2/(\beta-1)} + \delta^{-2/(\beta-1)}} \tag{14}$$

and $m_{i\emptyset} = 1 - \sum_{A_j \neq \emptyset} m_{ij}, \forall i = 1, n$ where $\alpha = 1$, $\beta = 2$, $\delta = 10$ is suggested in [10], and these parameter settings are used in this paper.

The aforementioned BBA determination approaches have shown their superiority in many applications [18]–[20] and they still have their own limitations in some area. Therefore, we propose to comprehensively use them through a learning mechanism.

IV. New Learning-based BBA Modeling Approach with Multi-method Fusion

If the prevailing BBA determination methods are jointly used, their pros could be promoted while their cons could be prohibited, and a better BBA modeling approach can be expected. To the comprehensive use of these methods more efficiently, we suggest to avoid explicitly using them in the test stage through a learning mechanism. In our approach, a deep network is trained to learn the mapping from the training samples to the corresponding comprehensive BBAs obtained by jointly using these methods as the generalized training labels. The BBAs of the test samples can be obtained in an end-to-end manner through the trained deep network model.

The proposed method mainly contains three stages, which is shown in Fig. 4.

1) The comprehensive BBAs as the generalized labels of the training samples are determined.

2) A deep network is trained to learn the end-to-end modeling of the BBA.

3) The BBAs of the test samples are obtained in an end-to-end manner through the trained network.

For the first stage in Fig. 4, the combined BBAs as the generalized labels are obtained through the combination of different BBAs determined by respectively using several prevailing BBA determination methods. In our approach, the BBA determination methods using interval number, the one using triangular fuzzy number, the one using trapezoidal fuzzy number and the ECM are used to determine different BBAs, respectively. Dempster's rule of combination is then used to fuse the different BBAs.

For the second stage in Fig. 4, the input of the network are the training samples while the output of the network are the corresponding combined BBAs as the generalized labels obtained in the first stage. Since deep learning is used in our approach, a crucial issue for training is to determine the loss function of the network. For our method, the aim of using the neural network is to learn the modeling of the BBA, and the loss function should properly measure the difference between the network's output and the combined BBA as the generalized label. Consequently, the evidence distance is used as the loss function since it specifically measures the dissimilarity between two BBAs. In this paper, Jousselme distance [21]

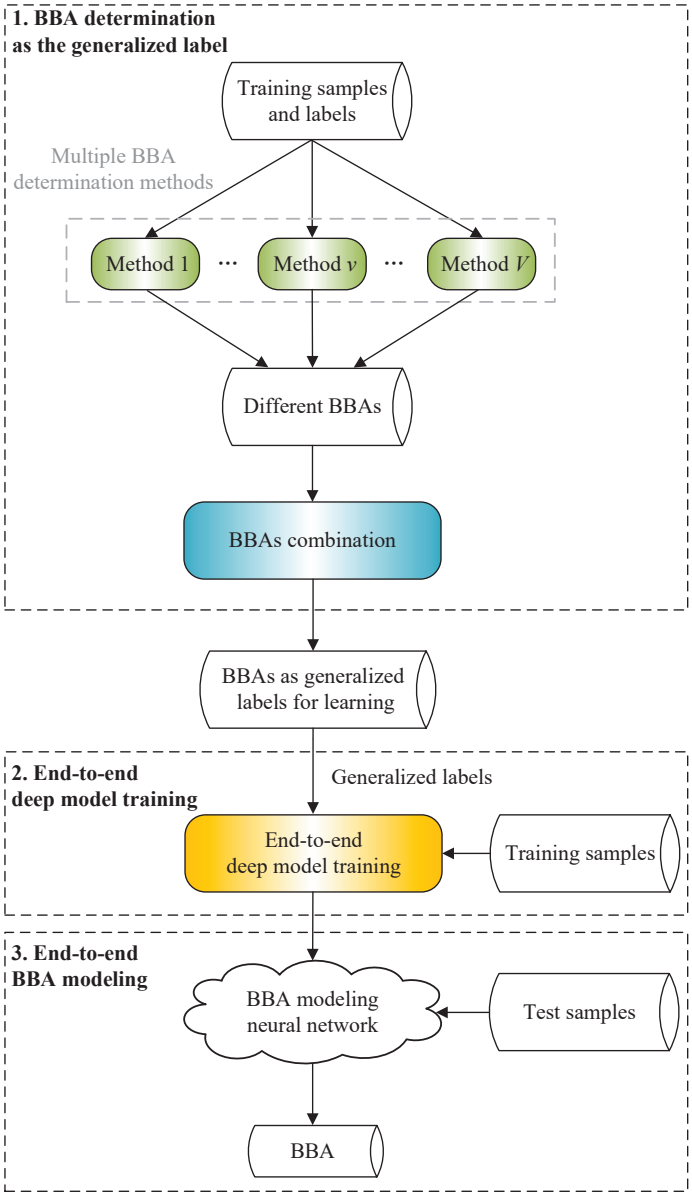

Fig. 4. Three stages of BBA modeling in our approach. In the first stage, the combined BBAs as the generalized labels are determined. In the second stage, an end-to-end network is trained. In the third stage, the network is used for the end-to-end BBA modeling.

is selected since it's one of the most widely used evidence distance, which is defined as:

$$d_J(m_1, m_2) = \sqrt{0.5 \cdot (m_1 - m_2)^T D (m_1 - m_2)} \quad (15)$$

where m_1 and m_2 are two independent BBAs be on the FOD Θ, D is Jaccard matrix

$$D(A, B) = \frac{|A \cap B|}{|A \cup B|} \quad (16)$$

where $A, B \subseteq \Theta$ and $A, B \neq \phi$, D is an $\left|2^{\Theta} - 1\right|$ dimension square matrix.

In order to make the output BBA more clear, which might benefit to the classification decision, the Ambiguity Measure (AM) [22] is used as a regularization term. The Ambiguity Measure is defined as:

$$AM(m) = -\sum_{\theta \in \Theta} BetP_m(\theta) \log_2 (BetP_m(\theta)) \quad (17)$$

where $BetP_m(\theta)$ is the probability obtained by the pignistic transformation.

Thus, the loss function used for the end-to-end deep model training is defined as follows:

$$Loss(\hat{m}, m) = d_J(\hat{m}, m) + \lambda \cdot AM(\hat{m}) \quad (18)$$

where m is the BBA as the generalized label, $\hat{m}$ is the model's output, λ is regularization coefficient and $\lambda = 0.05$ is used in this paper for the simplicity. Moreover, the regularization term is user-specified, one can try different regularization terms which fit the actual applications.

The specific network model is depend on the type of data. For the datasets only with few features, e.g., UCI datasets [23], a fully connected network is used in our work. For the image datasets, a more complex deep network should be used since the image contains richer information. ResNet18 [24] is used in this paper due to its good performance in handling image data.

To demonstrate the superiority of our approach, we compared the proposed method with several classic BBA determination methods on both UCI and some typical image datasets.

V. Experiments and Results

In our work, the 2-dimensional feature subspaces are used. Since the feature dimension of the samples we use is at least 5, the number of the 2-dimensional feature subspaces is at least $C_5^2 = 10$. Five feature subspaces are randomly selected from the training data, within which the BBAs are generated by the prevailing BBA determination approaches. These BBAs are then combined according to Dempster's rule, producing a aggregated BBA as the output BBA for each prevailing BBA determination method.

The proposed method LBMMF is compared with the BBA determination methods using interval number (IN), the one using triangular fuzzy number (TFN), the one using trapezoidal fuzzy number (TrFN) and the ECM. In each feature dimension, the percentiles of training samples are used in the fuzzy number-based BBA determination approaches. The 20th and 80th percentiles of the training samples in each feature dimension are used for modeling interval numbers. The 20th, 50th and 80th percentiles of the training samples in each feature dimension are used for modeling triangular fuzzy numbers. The 20th, 40th, 60th and 80th percentiles of the training samples in each feature dimension are used for modeling trapezoidal fuzzy numbers. The parameters for calculating similarity in Eqs. (5-9) are set as 5. The parameter settings $\alpha = 1$, $\beta = 2$, $\delta = 10$ are suggested in [10], which are used for ECM.

The methods are evaluated on 8 UCI [23] datasets (Appendicitis, Cancer, Ionosphere, Seeds, Vertebral, Wdbc, Wholesales and Wine) and 2 image datasets (CIFAR-10 [25] and

Weather [26]). For the CIFAR-10 dataset, we choose 4 classes for evaluation (cat, deer, dog, and horse). In each experiment, 60% samples are used as the training data and 40% samples are used as the test data. The experiments are repeated 100 times for UCI datasets and 20 times for image datasets. The mean evaluation metrics and their standard deviations on the test set are calculated from the results of these 100 (for UCI datasets) and 20 (for image datasets) repetitions.

We transform BBA into probabilities through Eq. (4) to obtain classification results. The classification results are then used to evaluate different BBAs, with classification accuracy, precision, recall and F1-score serving as the evaluation metrics. For the binary classification task, the accuracy, precision, recall and F1-score are defined as follows:

$$\text{Accuracy} = \frac{TP + TN}{TP + TN + FP + FN} \tag{19}$$

$$\text{Precision} = \frac{TP}{TP + FP} \tag{20}$$

$$\text{Recall} = \frac{TP}{TP + FN} \tag{21}$$

$$\text{F1-Score} = 2 \cdot \frac{\text{Precision} \cdot \text{Recall}}{\text{Precision} + \text{Recall}} \tag{22}$$

where TP represents the number of samples that the classifier correctly classifies the positive class; FN represents the number of samples that the classifier incorrectly classifies the negative class; FP represents the number of samples that the classifier incorrectly classifies the positive class; TN represents the number of samples that the classifier correctly classifies the negative class.

For the multi-class classification task, the accuracy is defined as follows:

$$\text{Accuracy} = \frac{N_{correct}}{N} \tag{23}$$

where N represents the number of samples, $N_{correct}$ represents the number of samples the classifier correctly classified. The precision, recall, and F1-score for multi-class classification are calculated as the average values of the respective metrics across all classes.

It is crucial to emphasize that the use of the classification performance aims specifically at evaluating different BBA modeling approaches, rather than using them for better classification results.

The evaluation metrics and the corresponding standard deviations using the BBAs determined by different approaches for classification are shown in Table II, and the highest metric for each row is in bold. The results are only used for the comparison of different BBA modeling approaches, which do not represent the best classification results of the corresponding datasets. We can find that using our approach to determine BBA generally achieves a better classification performance on both UCI and image datasets, which means LBMMF can model the BBA more properly. The reason for LBMMF achieves better results lies in the joint use of the prevailing BBA determination approaches. Moreover, the deep network well learns the mapping relationship from the training samples to the combined BBAs as the generalized training labels, which realize an efficient end-to-end BBA modeling for the test samples.

TABLE I
CONFUSION MATRIX FOR BINARY CLASSIFICATION TASK

		Predicted values	
		Positive	Negative
Actual values	Positive	TP	FN
	Negative	FP	TN

VI. Conclusion

In this paper, we proposed a novel approach for BBA modeling, termed Learning-based BBA Modeling with Multi-method Fusion (LBMMF), which jointly use the prevailing BBA determination methods through a learning mechanism. Our approach realizes an end-to-end BBA modeling for the test samples. The experiments on the classification applications have shown our approach can model BBA more properly than the compared methods. In future, we will focus on the joint use of multiple diverse BBA determination methods for better BBA modeling. For better joint use of multiple BBA determination methods, more combination rules, e.g., PCR6 [27] will be used. We will also use various evidence distances for further analysis and comparison. More appropriate uncertainty measures will be used as the regularization term.

References

[1] G. Shafer, *A mathematical theory of evidence*, vol. 42. Princeton university press, 1976.

[2] H. Zeng, B. Yang, X. Wang, J. Liu, and D. Fu, "Rgb-d object recognition using multi-modal deep neural network and ds evidence theory," *Sensors*, vol. 19, no. 3, p. 529, 2019.

[3] T. Grote and P. Berens, "Uncertainty, evidence, and the integration of machine learning into medical practice," in *The Journal of Medicine and Philosophy: A Forum for Bioethics and Philosophy of Medicine*, vol. 48, pp. 84–97, Oxford University Press US, 2023.

[4] A. Chowdhury, G. Karmakar, J. Kamruzzaman, R. Das, and S. S. Newaz, "An evidence theoretic approach for traffic signal intrusion detection," *Sensors*, vol. 23, no. 10, p. 4646, 2023.

[5] D. Han, Y. Yang, and C. Han, "Advances in ds evidence theory and related discussions," *Control and Decision*, vol. 29, no. 1, pp. 1–11, 2014.

[6] F. Selzer and D. Gutfinger, "Ladar and flir based sensor fusion for automatic target classification," in *Sensor fusion: Spatial reasoning and scene interpretation*, vol. 1003, pp. 236–246, SPIE, 1989.

[7] F. Valente and H. Hermansky, "Combination of acoustic classifiers based on dempster-shafer theory of evidence," in *IEEE International Conference on Acoustics, Speech and Signal Processing-ICASSP'07*, vol. 4, pp. IV–1129, IEEE, 2007.

[8] D. Han, J. Dezert, J.-M. Tacnet, and C. Han, "A fuzzy-cautious owa approach with evidential reasoning," in *15th International Conference on Information Fusion*, pp. 278–285, IEEE, 2012.

[9] W. Qiu and X. Liu, "Fuzzy time series model for forecasting based on dempster-shafer theory," *Control and Decision*, vol. 27, no. 1, pp. 99–103, 2012.

[10] M.-H. Masson and T. Denœux, "Ecm: An evidential version of the fuzzy c-means algorithm," *Pattern Recognition*, vol. 41, no. 4, pp. 1384–1397, 2008.

[11] B.-Y. Kang, Y. Li, Y. Deng, Y.-J. Zhang, and X.-Y. Deng, "Determination of basic probability assignment based on interval numbers and its application," *ACTA ELECTONICA SINICA*, vol. 40, no. 6, p. 1092, 2012.

TABLE II
CLASSIFICATION PERFORMANCE USING DIFFERENT BBA DETERMINATION METHODS (%)

Dataset	Metric	LBMMF	IN	TFN	TrFN	ECM
Appendicitis	Accuracy	**84.90 ± 4.72**	82.13 ± 5.47	81.93 ± 5.07	82.22 ± 5.08	79.47 ± 5.35
	Precision	**60.47 ± 5.33**	54.49 ± 5.96	53.77 ± 5.38	54.46 ± 5.62	49.07 ± 5.58
	Recall	71.85 ± 4.50	70.91 ± 5.39	73.15 ± 4.17	72.91 ± 4.45	**75.54 ± 3.84**
	F1-Score	**64.31 ± 3.06**	59.92 ± 4.25	60.65 ± 3.53	60.94 ± 3.59	58.41 ± 2.92
Cancer	Accuracy	**96.52 ± 1.18**	95.04 ± 1.51	95.52 ± 1.35	95.89 ± 1.23	93.14 ± 1.96
	Precision	**96.19 ± 1.75**	95.29 ± 2.09	95.41 ± 1.78	94.54 ± 2.08	94.36 ± 2.22
	Recall	**93.98 ± 2.79**	90.26 ± 4.28	91.58 ± 3.63	93.65 ± 3.04	83.70 ± 5.71
	F1-Score	**94.13 ± 1.76**	92.64 ± 2.46	93.41 ± 2.14	94.05 ± 1.87	89.39 ± 3.37
Ionosphere	Accuracy	**73.85 ± 3.40**	73.17 ± 4.28	72.19 ± 3.95	72.68 ± 4.30	71.29 ± 3.87
	Precision	**82.92 ± 4.98**	74.39 ± 6.52	78.86 ± 5.08	81.81 ± 5.33	77.46 ± 4.76
	Recall	81.51 ± 4.88	**83.22 ± 4.19**	71.90 ± 4.72	74.43 ± 4.95	78.19 ± 5.86
	F1-Score	**81.62 ± 5.68**	79.80 ± 5.65	76.60 ± 5.87	77.52 ± 6.01	77.95 ± 7.09
Seeds	Accuracy	**86.88 ± 3.84**	79.02 ± 4.35	80.97 ± 4.80	80.61 ± 4.92	85.80 ± 4.38
	Precision	**87.23 ± 3.78**	80.33 ± 5.94	83.13 ± 4.65	**87.23 ± 3.90**	82.48 ± 4.67
	Recall	**86.90 ± 3.59**	78.97 ± 4.01	80.92 ± 3.56	80.55 ± 3.68	85.80 ± 4.12
	F1-Score	**86.32 ± 4.00**	74.83 ± 4.89	77.81 ± 4.78	77.23 ± 4.09	84.17 ± 5.28
Vertebral	Accuracy	**71.93 ± 4.82**	70.58 ± 4.94	71.54 ± 4.85	71.31 ± 4.95	69.92 ± 4.06
	Precision	**69.70 ± 4.96**	68.76 ± 4.91	69.32 ± 4.98	69.10 ± 5.05	66.15 ± 4.23
	Recall	**70.75 ± 4.68**	70.10 ± 4.73	70.09 ± 4.59	70.09 ± 4.71	67.70 ± 4.18
	F1-Score	**67.82 ± 5.64**	66.39 ± 6.03	67.11 ± 5.74	66.92 ± 5.89	65.65 ± 4.39
Wdbc	Accuracy	**91.23 ± 3.32**	89.91 ± 4.08	89.46 ± 4.10	89.78 ± 4.04	90.12 ± 3.25
	Precision	90.27 ± 6.33	87.17 ± 7.33	84.26 ± 7.25	85.29 ± 7.32	**92.50 ± 5.28**
	Recall	**88.96 ± 4.37**	86.19 ± 5.29	86.99 ± 4.94	88.44 ± 4.49	80.13 ± 6.11
	F1-Score	**87.98 ± 4.38**	86.48 ± 5.03	86.37 ± 4.83	86.65 ± 4.85	85.73 ± 4.75
Wholesales	Accuracy	**86.61 ± 4.00**	82.72 ± 4.57	84.01 ± 4.92	84.09 ± 4.93	86.26 ± 4.94
	Precision	**82.95 ± 3.17**	75.05 ± 5.47	74.47 ± 5.55	75.02 ± 5.68	80.05 ± 5.85
	Recall	79.86 ± 3.63	79.07 ± 5.71	**81.50 ± 4.32**	80.81 ± 4.21	75.34 ± 4.32
	F1-Score	**79.36 ± 3.92**	75.81 ± 5.88	77.24 ± 4.76	77.20 ± 4.70	78.13 ± 5.38
Wine	Accuracy	**89.99 ± 3.39**	85.77 ± 4.46	86.46 ± 4.82	86.22 ± 4.95	86.90 ± 3.84
	Precision	**90.64 ± 3.09**	87.03 ± 3.06	87.40 ± 4.84	87.23 ± 3.92	87.31 ± 5.63
	Recall	**91.35 ± 3.50**	87.49 ± 3.28	88.04 ± 3.81	87.84 ± 3.92	88.03 ± 3.32
	F1-Score	**89.92 ± 3.88**	85.44 ± 4.04	86.25 ± 4.17	85.97 ± 4.38	86.99 ± 4.92
CIFAR-10*	Accuracy	**93.04 ± 2.74**	90.92 ± 4.89	91.91 ± 4.50	91.77 ± 4.55	91.36 ± 2.21
	Precision	**93.02 ± 2.55**	91.59 ± 3.54	92.14 ± 3.84	92.00 ± 4.01	91.05 ± 2.19
	Recall	**92.39 ± 3.03**	89.87 ± 5.40	91.04 ± 4.96	90.87 ± 5.03	90.69 ± 2.42
	F1-Score	**92.37 ± 3.22**	89.51 ± 7.18	90.79 ± 6.31	90.59 ± 6.50	90.59 ± 2.47
Weather	Accuracy	**94.76 ± 2.63**	93.50 ± 3.71	93.63 ± 3.21	93.69 ± 3.33	92.58 ± 2.51
	Precision	**94.65 ± 2.49**	93.60 ± 3.18	93.66 ± 2.83	93.75 ± 2.93	92.56 ± 2.25
	Recall	**94.97 ± 2.58**	93.80 ± 3.58	93.93 ± 3.12	93.99 ± 3.23	92.91 ± 2.49
	F1-Score	**94.60 ± 2.73**	93.35 ± 3.84	93.51 ± 3.30	93.57 ± 3.43	92.41 ± 2.58

*Four classes are used (cat, deer, dog, and horse).

[12] Z. Zhang, D. Han, J. Dezert, and Y. Yang, "Determination of basic belief assignment using fuzzy numbers," in *20th International Conference on Information Fusion (Fusion)*, pp. 1–6, 2017.

[13] Y. Tang, D. Wu, and Z. Liu, "A new approach for generation of generalized basic probability assignment in the evidence theory," *Pattern Analysis and Applications*, vol. 24, pp. 1007–1023, 2021.

[14] M. C. Florea, A.-L. Jousselme, D. Grenier, and É. Bossé, "Approximation techniques for the transformation of fuzzy sets into random sets," *fuzzy sets and systems*, vol. 159, no. 3, pp. 270–288, 2008.

[15] D. Han, C. Han, and Y. Deng, "Novel approaches for the transformation of fuzzy membership function into basic probability assignment based on uncertainty optimization," *International Journal of Uncertainty, Fuzziness and Knowledge-Based Systems*, vol. 21, no. 02, pp. 289–322, 2013.

[16] P. Smets and R. Kennes, "The transferable belief model," *Classic Works of the Dempster-Shafer Theory of Belief Functions*, pp. 693–736, 2008.

[17] L. Tran and L. Duckstein, "Comparison of fuzzy numbers using a fuzzy distance measure," *Fuzzy sets and Systems*, vol. 130, no. 3, pp. 331–341, 2002.

[18] L. Zheng and F. Xiao, "Complex interval number-based uncertainty modeling method with its application in decision fusion," *International Journal of Intelligent Systems*, vol. 37, no. 12, pp. 11926–11943, 2022.

[19] L. Jiao, F. Wang, Z.-g. Liu, and Q. Pan, "Tecm: Transfer learning-based evidential c-means clustering," *Knowledge-Based Systems*, vol. 257, p. 109937, 2022.

[20] N. Makni, N. Betrouni, and O. Colot, "Introducing spatial neighbourhood in evidential c-means for segmentation of multi-source images: Application to prostate multi-parametric mri," *Information Fusion*, vol. 19, pp. 61–72, 2014.

[21] A.-L. Jousselme, D. Grenier, and É. Bossé, "A new distance between two bodies of evidence," *Information fusion*, vol. 2, no. 2, pp. 91–101, 2001.

[22] A.-L. Jousselme, C. Liu, D. Grenier, and É. Bossé, "Measuring ambiguity in the evidence theory," *IEEE Transactions on Systems, Man, and Cybernetics-Part A: Systems and Humans*, vol. 36, no. 5, pp. 890–903, 2006.

[23] M. Lichman *et al.*, "Uci machine learning repository," 2013.

[24] K. He, X. Zhang, S. Ren, and J. Sun, "Deep residual learning for image recognition," in *Proceedings of the IEEE conference on computer vision and pattern recognition*, pp. 770–778, 2016.

[25] A. Krizhevsky, G. Hinton, *et al.*, "Learning multiple layers of features from tiny images," 2009.

[26] A. Gbeminiyi, "Multi-class weather dataset for image classification," *Mendeley Data*, vol. 6, pp. 15–23, 2018.

[27] F. Smarandache and J. Dezert, "On the consistency of pcr6 with the averaging rule and its application to probability estimation," in *Proceedings of the 16th International Conference on Information Fusion*, pp. 1119–1126, IEEE, 2013.